Biogeosciences Discuss., 9, 10645–10668, 2012
www.biogeosciences-discuss.net/9/10645/2012/
doi:10.5194/bgd-9-10645-2012

Biogeosciences Discussions

Response of bacterioplankton community structure to an artificial gradient of pCO_2 in the Arctic Ocean

R. Zhang[1,*], X. Xia[1,*], S. C. K. Lau[2], C. Motegi[3], M. G. Weinbauer[3], and N. Jiao[1]

[1]State Key Laboratory of Marine Environmental Science, Xiamen University, Xiamen 361005, China
[2]Division of Life Science and Division of Environment, The Hong Kong University of Science and Technology, Clear Water Bay, Kowloon, Hong Kong SAR, China
[3]Microbial Ecology and Biogeochemistry Group, Université Pierre et Marie Curie-Paris 6, CNRS, Laboratoire d'Océanographie de Villefranche, 06230 Villefranche-sur-Mer, France
[*]These authors contributed equally to this work.

Received: 28 July 2012 – Accepted: 30 July 2012 – Published: 9 August 2012

Correspondence to: N. Jiao (jiao@xmu.edu.cn) and M. G. Weinbauer (wein@obs-vlfr.fr)

Published by Copernicus Publications on behalf of the European Geosciences Union.

Abstract

The influences of ocean acidification on bacterial diversity were investigated using DNA fingerprinting and clone library analysis of bacterioplankton samples collected from the largest CO_2 manipulation mesocosm study that had been performed thus far. Terminal restriction fragment length polymorphism analysis of the PCR amplicons of the 16S rRNA genes revealed that bacterial diversity, species richness and community structure varied with the time of incubation but not the degree of ocean acidification. The phylogenetic composition of the major bacterial assemblage after a 30-day incubation under various pCO_2 concentrations did not show clear effects of pCO_2 levels. However, the maximum apparent diversity and species richness which occurred during incubation differed in the high and low pCO_2 treatments, in which different bacterial community structure harbored. In addition, total alkalinity was one of the contributing factors for the temporal variations in bacterial community structure observed during incubation. A negative relationship between the relative abundance of *Bacteroidetes* and pCO_2 levels was observed for samples at the end of the experiment. Our study suggested that ocean acidification affected the development of bacterial assemblages and potentially impacts the ecological function of the bacterioplankton in the marine ecosystem.

1 Introduction

Microorganisms are a key component in marine planktonic food webs (Amann et al., 1995). The phytoplankton and cyanobacteria contribute significantly to photosynthesis and primary production. Heterotrophic bacteria and archaea maintain the productivity by the recycling of organic and inorganic nutrients. These microbial functions are crucial components in several major oceanic models, e.g. the microbial loop (Amann et al., 1995) and microbial carbon pump (Jiao et al., 2010).

Generally, microbial diversity and community structure are controlled by abiotic and biotic factors. For example, bacterial communities are affected by the spatial and

BGD
9, 10645–10668, 2012

temporal dynamics of environmental parameters. Nutrient availability and water characteristics (e.g. temperature, salinity and pH) contribute to microbial biogeography in the ocean (Martiny et al., 2006). Considering the changing oceanic conditions induced by anthropogenic impacts (including climate change), it is necessary to investigate whether and how the microbial communities would respond to the emerging changes, and also to evaluate the possible ecological consequences of the microbial responses. Such hitherto unknown information is crucial to our understanding and to predictions of the possible effects of global climate changes to the biosphere (IPCC, 2007).

A consequence of increasing atmospheric CO_2 to the ocean is acidification of the water, which has been confirmed by long term field observation and undoubtedly related to anthropogenic CO_2 emission (Dore et al., 2009). It is estimated that the pH of seawater would be decreased by 0.2 to 0.4 units by the end of this century (Caldeira and Wickett, 2003). This predicted rate of ocean acidification is greater than those that have occurred over the past 300 million years (Hönisch et al., 2012). Such changes would fundamentally alter ocean chemistry from the surface water to the deep sea. Our understanding of the biological and ecological effects of changing seawater carbonate chemistry is still in its infancy. While it is well recognized that ocean acidification will have serious negative impacts for most marine calcifiers, the increasing pCO_2 effects on non-calcifers are not clear. For example, positive effects of elevated CO_2 concentration are observed for marine autotrophs in the phytoplankton (Riebesell, 2004), suggesting a "CO_2 fertilization" phenomenon (Hutchins et al., 2009). While similar fertilization effects occur for the cyanobacteria *Synechococcus*, the other major cyanobacteria *Prochlorococcus* shows no response to CO_2 increase (Fu et al., 2007). It appears that autotrophic nitrogen fixers and anaerobic denitrifiers directly or indirectly benefit from ocean acidification (Hutchins et al., 2007, 2009). However, the abundance and/or activity of nitrifers might be depressed since nitrification rates decline with rising CO_2 level in the ocean (Beman et al., 2011).

Thus far, most of our knowledge of ocean acidification on microbes is derived from laboratory experiments with a small number of cultured microbial taxa (Liu et al.,

BGD
9, 10645–10668, 2012

2010a), and knowledge about the response of natural heterotrophic bacterioplankton communities to ocean acidification is scarce. In a mesocosm study, Grossart et al. (2006) find that pCO_2 level positively impacts bacterial production but not bacterial abundance. In addition, the coupling of heterotrophic bacteria and phytoplankton occurs at different pCO_2 levels (Allgaier et al., 2008). The only study of bacterial community structure response to ocean acidification indicates that free-living bacteria, but not particle-attached ones, develop dependent on the pCO_2 level (Allgaier et al., 2008).

In the current study, we used DNA fingerprinting and clone library analysis to investigate the dynamics of bacterial diversity and community structure during the 30-day EPOCA mesocosm experiment in Arctic waters, which is the largest ocean acidification experiment performed so far (Riebesell et al., 2012). Together with the investigation of other bacterial process parameters (e.g. bacterial production, respiration), our study provided, for the first time, detailed information on the responses of bacterial diversity to ocean acidification.

2 Materials and methods

2.1 Experimental set up and sampling

The experimental setup and the methods for the monitoring of core environmental parameters (e.g. nutrients and chl *a*) are provided in details elsewhere in this issue (Schulz et al., 2012). Nine mesocosms were prepared and stepwise addition of CO_2 saturated seawater was applied to obtain different levels of pCO_2. The mean pCO_2 values of each mesocosm during the experiment were 175 (M3), 180 (M7), 250 (M2), 340 (M4), 425 (M8), 600 (M1), 675 (M6), 860 (M5) and 1085 (M9) µatm. Seawater samples for the analysis of bacterial community structure were obtained from the mesocosms using Hydrobios integrated water samplers. Nineteen sampling events were performed over the entire 30-day period of the mesocosm experiment. Nutrients were added into all mesocosms prior to the sampling on day 13 in order to induce the development of

BGD
9, 10645–10668, 2012

a phytoplankton bloom (Schulz et al., 2012). Microbial cells in freshly collected seawater samples (2 l each) were harvested using membrane filtration (0.22-µm-pore-size Isopore membrane, Millipore). The membranes were stored at −20 °C until DNA extraction.

2.2 DNA extraction and PCR amplification of bacterial 16S rRNA genes

DNA was extracted following a protocol in Zhang et al. (2007) with some modifications. The filter membranes were deep frozen and thawed three times in liquid N_2 and at 65 °C, respectively. Eight µl of proteinase K (10 mg ml^{-1} in TE buffer) was then added, followed by incubation for 30 min at 37 °C. After that, 80 µl of 20 % SDS was added, followed by incubation for 2 h at 65 °C. After vortexing, an equal volume of phenol-chloroform-isoamylalcohol (25 : 24 : 1 by volume) was added and the mixture centrifuged at 10 000 g for 5 min. The aqueous phase was extracted using a chloroform-isoamylalcohol (24 : 1 by volume) mixture and centrifugation. Subsequently, a 0.6 times volume of isopropanol was added to the aqueous solution and it was incubated for 20 min, and then centrifuged at 12 000 g for 15 min. The DNA was washed with 70 % ethanol and dissolved in 100 µl of double-distilled water.

The amplification of bacterial 16S rRNA genes for DNA fingerprinting analysis was performed with universal primers 27F (5′-AGA GTT TGA TCC TGG CTC AG-3′), fluorescently labeled with 6-carboxyfluorescein phosphoramidite (Fam), and 907R (5′-CCG TCA ATT CMT TTG AGT TT-3′) (Amann et al., 1995). Each PCR mixture (50 µl) contained 5 µl PCR buffer, 200 µM of each deoxynucleoside triphosphate, 0.1 µM of each primer, ∼ 10 ng of template DNA, and 0.5 U of Ex-Taq DNA polymerase (TAKARA). The thermal cycles were 95 °C for 3 min; 30 cycles of 95 °C for 1 min, 55 °C for 1 min, 72 °C for 1 min; and 72 °C for 10 min. PCR products were purified using the QIAquick PCR Purification Kit (Qiagen) according to the manufacturer's protocol.

BGD
9, 10645–10668, 2012

2.3 Terminal restriction fragment length polymorphism (T-RFLP) analysis

Purified PCR products were double-digested with restriction enzymes Msp I and Rsa I (NEB) according to the manufacturer's protocol. Selected samples were digested only with Rsa I so as to verify that the T-RFLP patterns obtained were the result of double digestion. Aliquots of digested PCR products were mixed with 0.125 µl of the internal size standard (MapMarker1000, BioVentures) and analyzed using the MegaBACE platform (Amersham). All T-RF analyses were performed using the Genetic Profiler in the MegaBACE software package (Amersham) in accordance with Lau et al. (2005). T-RFs < 50 bp and > 900 bp were excluded from the analysis to avoid detection of primers and uncertainties of size determination, respectively. T-RFs with a peak area less than 1 % of the total peak area of each sample were removed for statistical analysis. An improved binning strategy was applied for the T-RFLP data matrix following the protocol described previously (Hewson and Fuhrman, 2006). The resultant T-RF data were analyzed using PRIMER 5 software (Clarke and Gorley, 2001). MDS (multidimensional scaling) analyses were based on Log $(x+1)$ transformation of percentage values and Euclidean distance. The Shannon-Weaver index (H) was calculated as:

$$H = -\sum (P_i \cdot \log P_i)$$

where $P_i = n_i\ N^{-1}$, n_i is the area of a peak and N is the sum of all peak areas in each sample. The relationship between the measured environmental parameters (Schulz et al., 2012) and the bacterial community structure revealed by T-RFLP was studied using the BIOENV analysis provided in PRIMER 5 software. BIOENV analysis was used to select the environmental parameters that may best explain the community pattern (presence/absence and area of T-RFs), maximizing the correlation between their respective similarity matrices with application of a weighted Spearman's correlation coefficient.

BGD
9, 10645–10668, 2012

2.4 Clone library construction and phylogenetic analysis

The bacterial 16S rRNA genes in the day 30 samples were PCR amplified using the primer set 27F and 1492R (5′-GGC TAC CTT GCC ACG ACT TC-3′) with the same PCR program as described above (Lane, 1991) The PCR amplicons (~ 1500 bp in size) were cloned into the vector with a TOPO TA Cloning Kit (Invitrogen) according to the manufacturer's instructions. The 16S rRNA genes were sequenced from both ends using the primers M13F and M13R on an ABI DNA autosequencer. Phylogenetic affiliations of the sequences were determined using the BLASTN program on the NCBI website (http://www.ncbi.nlm.nih.gov) and RDP (http://rdp.cme.msu.edu/). The DNA sequences obtained in this study are available from GenBank under the accession numbers JN975970-JN976712. The possible phylogenetic assignment of T-RFs from T-RFLP analysis of environmental samples was performed with in silico digestion of the DNA sequence of each clone. A variation of 1–3 bp, depending on the size of the T-RF, was applied for the comparison between T-RF positions of community-based and sequence-based in silico analysis (Liu et al., 2010b).

3 Results

3.1 Bacterial community dynamics revealed using T-RFLP analysis

The T-RFLP patterns obtained for the nine mesocosms at each time point of sampling were generally quite similar (e.g. see Fig. 1 for the eight T-RFLP patterns of day 30 samples. The M7 sample is absent since the mesocosm was removed before day 30). The numbers and positions of T-RFs were similar among mesocosms, although the peak heights varied. As a result, MDS analysis of the T-RFLP patterns with double enzyme digestion showed no clear distinction between samples from each individual mesocosm (Fig. 2a). This was verified using T-RFLP analysis with single enzyme digestion (Msp I, Fig. S1a). On the contrary, the MDS plots of T-RFLP analysis with double or

BGD
9, 10645–10668, 2012

single enzyme digestion revealed temporal patterns of bacterial communities during the 30-day incubation (Figs. 2b and S1b). The bacterial community structure gradually changed with the incubation period. Samples collected at adjacent dates grouped together on the MDS plot while the most distinctive comparisons were those from the onset and termination of the experiment (Figs. 2b and S1b). This pattern (clear temporal but no pCO_2 effect) observed in MDS plots was also shown with ANOSIM analysis based on the matrix of T-RF position and peak area (Tables S1 and S2).

Three phases, respective to chl *a* concentration, were observed during the mesocosm experiments (Schulz et al., 2012). Phase 1 included from manipulation to nutrient addition (day 13), the first chl *a* minimum period. This was followed by Phase 2 (day 13–day 21) until the second chl *a* minimum. Phase 3 (day 22–day 30) seemed to be uncompleted when the experiment was terminated. Apparent species richness (number of T-RFLPs in each sample) and Shannon-Weaver diversity index calculated using the T-RFLP matrix, also showed three phases (Fig. 3). However, the rhythmicity of chl *a* concentration and bacterial diversity were different.

Generally, the apparent bacterial species richness and diversity index increased rapidly during the CO_2 manipulation procedure, peaked at around day 3–day 5 and then decreased until day 10. The first peak and trough of apparent bacterial diversity were ahead of those observed in terms of the chl *a* concentration. Then these two parameters increased again until day 20–day 24. The second peak and trough of apparent bacterial diversity were delayed compared to chl *a*. During the last several days, they were at the beginning of the third phase until the termination of the experiment, which was similar to chl *a* but the amplitude was smaller (Fig. 3). Similar to the chl *a* pattern, the minimum apparent bacterial diversity and species richness gradually increased during the whole experimental period.

The maximum species richness (S_{max}) and diversity index (H_{max}), which occurred in the different treatments during the incubation period, varied from 27–35 and 2.725–3.18, respectively (Fig. 4a). Significant differences of S_{max} (independent t-test, $p = 0.039$) and H_{max} (independent t-test, $p = 0.005$) were observed between the three

BGD
9, 10645–10668, 2012

highest pCO_2 treatments (M6, 5, 9) and other medium (M4, 8, 1) and low pCO_2 treatments (M3, 7, 2). The S_{max} (27–29) and H_{max} values (2.725–2.906) in the three highest pCO_2 treatments were lower than in the other treatments. MDS plotting of the samples with maximum bacterial diversity showed that samples from three highest pCO_2 treatments were grouped together but were separated from the other samples (Fig. 4b).

BIOENV analysis was applied to investigate the potential effects of environmental parameters on the observed bacterial community structure (Table 1). Generally, the correlation between bacterial community structure and measured environmental factors was low. The highest correlation (0.452) was obtained with combined environmental factors including salinity, dissolved oxygen (DO) concentration, bacterial abundance (BA), viruses-to-bacteria ratio (VBR) and dimethylsulfide (DMS)/particulate organic nitrogen (PON) concentration. Other parameters listed as contributors were particulate organic carbon (POC) and total alkalinity (A_T) (Table 1). Considering individual factors, the five parameters, which correlated best with community composition, were salinity, DO, BA, A_T and DMS. The detailed information about these parameters is provided elsewhere in this issue (Schulz et al., 2012).

3.2 Bacterial community composition revealed by clone library analysis

In total, 743 clones were obtained from eight clone libraries (74–100 clones each) constructed from the samples collected on day 30 (Table 2). Sequences of *Proteobacteria*, *Actinobacteria* and *Bacteroidetes* dominated all clone libraries. At the family level, the *Microbacteriaceae*, *Rhodobacteraceae* and *Alteromonadaceae* were the major groups. Based on a definition of operational taxonomic units (OTU) as 97 % similarity of the 16S rRNA gene sequence, there were 13–27 OTUs in each clone library (Fig. S2). The phylogenetic assignment and number of clones of each OTU are shown in Table 2. *Cryobacterium*-like, *Haliea*, *Ilumatobacter*, *Sulfitobacter* and *Loktanella* related OTUs were the five most abundant ones. We did not observe a clear trend of apparent bacterial diversity (number of OTUs) versus pCO_2 concentrations (data not shown). Although Libshuff analysis showed significant difference in various pair comparisons

BGD
9, 10645–10668, 2012

of the clone library, there was no statistical evidence suggesting a pCO_2-related effect (Table S3). The difference among clone libraries was probably related to the fact that the relatively small sampling size (< 100 clones) in the clone library analysis was insufficient to capture the true diversity, as shown by the unsaturated asymptotic rarefaction curves in Fig. S2. Similar to the T-RFLP analysis, rarefaction analysis did not reveal clear diversity changes along the pCO_2 gradient.

Although the relative abundance of most OTUs revealed using clone library analysis did not show clear pCO_2 effects (Table 2), some OTUs seemed to be affected by pCO_2 levels. For example, *Polaribacter* OTUs (*Bacteroidetes*) were only found in the four lowest pCO_2 mesocosms but not in the four highest pCO_2 treatments. In contrast, we observed highest abundance of *Pelagibacter* OTU (*Alphaproteobacteria*) in the higher pCO_2 mesocosms.

The obtained sequences were in silico digested using the restriction enzymes Msp I and Rsa I for possible phylogenetic assignment to the T-RFs observed for day 30 samples. In total, we successfully identified six major T-RFs (see Fig. 1 for their positions), accounting for 73.8–86.6 % of the total peak area of each sample (Fig. 5). A T-RF of 72–75 bp was the largest peak (44.2 ± 14.9 % of total peak area, $n = 8$) in all day 30 samples, especially in Mesocosm 9 (Figs. 1 and 5). The e-digestion analysis of clone library sequences suggested that two *Actinobacteria* groups (*Ilumatobacter* and *Cryobacterium*) produced this T-RF. This was supported by the finding that the clone libraries were dominated by clones affiliated in these two *Actinobacteria* groups (Table 2). Several *Bacteroidetes* sequences (*Polaribacter*, *Ulvibacter*, *Haliscomenobacter* and *Owenweeksia*) produced two major T-RFs located at 86–92 bp and 308–313 bp. A negative linear correlation ($R^2 = 0.60$) between the relative abundance of *Bacteroidetes* T-RFs and pCO_2 levels was observed. The T-RFs at 420–424 bp and 436–440 bp probably originated from the Alphaproteobacteria *Sulfitobacter* and *Loktanella*, respectively. The second most abundant OTU (*Haliea* of the *Gammaproteobacteria*) in the clone library contributed to the T-RF of 485–488 bp (Figs. 1 and 5).

BGD
9, 10645–10668, 2012

There was no clear trend of relative abundance of *Alphaproteobacteria* (individual or combined) and *Gammaproteobacteria* along the gradient of pCO_2 levels.

4 Discussion

4.1 Temporal effects on bacterial community structure

Generally, MDS analysis of T-RFLP patterns revealed significant temporal variations of bacterial community structure. Although an investigation of the temporal dynamics of bacterial community was not the main objective in the current experimental design, this suggested that environmental changes, which commonly occurred in all mesocosms, controlled the dynamics of bacterial communities during incubation. In addition, nutrient manipulation at the middle of the experiment, which induced higher productivity in the mesocosm, could also contribute to the temporal pattern observed for bacterial community structure. Coupling of the bacterial community and the phytoplankton is frequently observed in natural or experimental systems (Allgaier et al., 2008; Azam et al., 1983; Duarte et al., 2005). Labile dissolved organic matter (DOM, e.g., photosynthetic extracellular release) affects bacterial biomass, production and community structure. In the present study, the trend of apparent bacterial diversity and species richness seemed to be independent of chl *a* development before nutrient addition (Phase 1), while it co-varied with the development of chl *a* after nutrient addition (Phases 2 and 3) (Figs. 3 and Schulz et al., 2012), indicating a potential influence of the phytoplankton on bacterial community development. Furthermore, DMS, which is mainly produced by phytoplankton, was listed as one of the best correlated environmental factor combinations for bacterial community structure. Therefore, our study suggested that autotrophic phytoplankton might strongly contribute to heterotrophic bacterial community development, which was related to nutrient stimulation, as well as pCO_2 manipulation, during incubation (Bellerby et al., 2012).

BGD
9, 10645–10668, 2012

4.2 The effects of pCO_2 on bacterial community structure

The lack of any observed pCO_2 effect on community composition as assessed using T-RFLP and small clone libraries seemed to support the null hypothesis, raised by Joint et al. (2010), that the general bacterial community is not fundamentally different under higher CO_2/low pH conditions. Huge bacterial diversity, genetic plasticity and acclimation with existing cell machinery can result in the stability of a bacterial community in high CO_2/low pH environments (Joint et al., 2010). However, T-RFLP and small clone library analyses detected less than 50 T-RFs and OTUs, respectively. Only major phylogenetic groups, not rare species (which provide the majority of bacterial diversity), can be detected using these techniques. In addition, micro-diversity of bacteria (e.g. those which have less than 1 % difference in 16S rRNA gene sequence but show distinctive ecological functions) would not be detected using these techniques. This might prevent the detection of possible pCO_2 effects at the general diversity level. BIOENV analysis suggested that salinity, DO, BA, VBR and DMS or PON were the major factors contributing to the dynamics of general bacterial community dynamics. Also, one parameter (A_T), which is directly related with CO_2 manipulation, was listed as a possible contributor to bacterial community dynamics. This indicated that pCO_2 and its chemical consequences in the ocean might not be the direct forces responsible for the main structure of the bacterial assemblage. However, pCO_2 effects were observed for S_{max} and H_{max} during incubation (Fig. 4). At high pCO_2 S_{max} and H_{max} were reduced and indicated a threshold of pCO_2 concentration between 600–675 µatm which caused observed bacterial community responses to ocean acidification. Furthermore, a pCO_2 related chemical parameter A_T was suggested, using BIOENV analysis, to affect bacterial community structure. This evidence proved the potential influence of ocean acidification on the development of bacterial communities, although the general community structures of the bacterioplankton were quite stable.

Metagenomic analysis along a vertical profile in the oligotrophic ocean showed that representatives of the *Alphaproteobacteria* and the *Gammaproteobacteria* are

BGD
9, 10645–10668, 2012

distributed in waters covering a wide range of natural pH conditions (DeLong et al., 2006). In our study, the relative abundance of *Alphaproteobacteria* and *Gammaproteobacteria*, revealed using T-RFLP analysis, did not vary with the level of acidification, suggesting that these two dominating marine bacterial phylogenetic groups had enough genetic or metabolic plasticity to compensate for lower pH conditions. However, considering the contrasting distribution of *Polaribacter* and *Pelagibacter* in the clone library analysis, there were possibilities that ocean acidification might have depressed or stimulated some phylogenetic lineages in the *Alphaproteobacteria* and *Gammaproteobacteria*.

A negative relationship between pCO_2 level and relative abundance (peak area) of *Bacteroidetes* T-RFs was observed in our study. *Bacteroidetes* is an important consumer of high molecular weight (HMW) DOM in the ocean (Kirchman, 2002). They are major heterotrophic inhabitants on marine particles as well, contributing to the degradation of particulate organic matter (POM) (Zhang et al., 2007). Ocean acidification potentially affects the production of POM, DOM and other organic matter, e.g. transparent exopolymer particles (Liu et al., 2010a). Few studies have investigated the fate of organic matter in the acidified ocean. Piontek et al. (2010) observe increased degradation of polysaccharides during acidification. However, if our observation was correct, this could in the future significantly influence ocean marine carbon cycling. For example, the possible stimulation of POM production and the decline of their heterotrophic consumers (e.g. *Bacteroidetes*) might enhance the biological carbon pump and carbon sequestration in the ocean. Meanwhile, microbial populations with reduced *Bacteroidetes* might leave more HMW DOM in the sea water, thus affecting the efficiency of the microbial carbon pump and possibly increasing carbon storage in the ocean (Jiao et al., 2010). It is clear that attention to the influence of ocean acidification on microbial mediated marine carbon cycling (e.g. the biological pump and microbial carbon pump) should be a priority in global change studies.

Within the same mesocosms, the eukaryotic phytoplankton was stimulated by higher pCO_2 manipulations (Schulz et al., 2012). Interestingly, based on clone library analysis,

BGD
9, 10645–10668, 2012

we did not find consistent stimulation effects of higher pCO_2 on the cyanobacteria, the other autotrophic group in the Arctic Ocean, which is contradictory to previous laboratory study based on cyanobacterial isolates (Fu et al., 2007). Although this might be due to the low abundance of cyanobacteria in the in situ Arctic environment, our study showed the possible discrepancy between field investigation and laboratory study, which should lead to caution in applying conclusions from cultured organisms to the natural ecosystem.

5 Outlook

Our study shed light on the ocean acidification effects on bacterial community structure in the Arctic Ocean, demonstrating a general resilience of the major bacterial phylogenetic groups under various higher pCO_2 conditions. However, specific bacterial lineages responded to elevated pCO_2 concentrations. Therefore, higher resolution techniques (e.g. 454 pyrosequencing or microarray analyses) should be applied in the future in order to detect any subtle but ecologically significant changes of bacterioplankton diversity to elevated pCO_2 levels. Furthermore, considering the tight coupling of the heterotrophic bacteria and the phytoplankton in our mesocosm study, pCO_2 manipulation experiments performed without autotrophs are needed to elucidate the pure response of the bacteria to ocean acidification.

Supplementary material related to this article is available online at: http://www.biogeosciences-discuss.net/9/10645/2012/bgd-9-10645-2012-supplement.pdf.

Acknowledgements. This work is a contribution to the "European Project on Ocean Acidification" (EPOCA) which received funding from the European Community's Seventh Framework Programme (FP7/2007-2013) under grant agreement no. 211384. We gratefully acknowledge

BGD
9, 10645–10668, 2012

the logistical support of Greenpeace International for its assistance with the transport of the mesocosm facility from Kiel to Ny-Ålesund and back to Kiel. We also thank the captains and crews of M/V ESPERANZA of Greenpeace and R/V *Viking Explorer* of the University Centre in Svalbard (UNIS) for assistance during mesocosm transport and during deployment and recovery in Kongsfjorden. We thank the staff of the French-German Arctic Research Base at Ny-Ålesund, in particular Marcus Schumacher, for on-site logistical support. Financial support was provided by the 973 program (2011CB808800) and NSFC (40906059) of China. R. Z. was supported by the Program for New Century Excellent Talents in University (NCET 09-0683). We gratefully acknowledge the help provided by the Chinese Arctic and Antarctic Administration, SOA (IC2010006). Financial support was provided by IPEV, The French Polar Institute John Hodgkiss is thanked for his help in polishing the English in this manuscript.

References

Allgaier, M., Riebesell, U., Vogt, M., Thyrhaug, R., and Grossart, H.-P.: Coupling of heterotrophic bacteria to phytoplankton bloom development at different pCO_2 levels: a mesocosm study, Biogeosciences, 5, 1007–1022, doi:10.5194/bg-5-1007-2008, 2008.

Amann, R. I., Ludwig, W., and Schleifer, K. H.: Phylogenetic identification and in situ detection of individual microbial cells without cultivation, Microbiol. Mol. Biol. R., 59, 143–169, 1995.

Azam, F., Fenchel, T., Field, J. G., Gray, J. S., Meyer-Reil, L. A., and Thingstad, F.: The ecological role of water-column microbes in the sea, Mar. Ecol.-Prog. Ser., 10, 257–263, 1983.

Bellerby, R. G. J., Silyakova, A., Nondal, G., Slagstad, D., Czerny, J., De Lange, T., and Ludvig, A.: Marine carbonate system evolution during the EPOCA Arctic pelagic ecosystem experiment in the context of simulated future Arctic ocean acidification, in preparation, 2012.

Beman, J. M., Chow, C. E., King, A. L., Feng, Y., Fuhrman, J. A., Andersson, A., Bates, N. R., Popp, B. N., and Hutchins, D. A.: Global declines in oceanic nitrification rates as a consequence of ocean acidification, P. Natl. Acad. Sci. USA, 108, 208–213, 2011.

Caldeira, K. and Wickett, M. E.: Anthropogenic carbon and ocean pH, Nature, 425, p. 365, 2003.

Clarke, K. R. and Gorley, R. N.: PRIMER v5: User Manual/Tutorial, PRIMER-E Ltd, Plymouth, UK, 2001.

DeLong, E. F., Preston, C. M., Mincer, T., Rich, V., Hallam, S. J., Frigaard, N.-U., Martinez, A., Sullivan, M. B., Edwards, R., Brito, B. R., Chisholm, S. W., and Karl, D. M.: Community

BGD

9, 10645–10668, 2012

genomics among stratified microbial assemblages in the ocean's interior, Science, 311, 496–503, doi:10.1126/science.1120250, 2006.
Dore, J. E., Lukas, R., Sadler, D. W., Church, M. J., and Karl, D. M.: Physical and biogeochemical modulation of ocean acidification in the Central North Pacific, P. Natl. Acad. Sci. USA, 106, 12235–12240, 2009.
Duarte, C. M., Agustí, S., Vaqué, D., Agawin, N. S. R., Felipe, J., Casamayor, E. O., and Gasol, J. M.: Experimental test of bacteria-phytoplankton coupling in the Southern Ocean, Limnol. Oceanogr., 50, 1844–1854, 2005.
Fu, F. X., Warner, M. E., Zhang, Y., Feng, Y., and Hutchins, D. A.: Effects of increased temperature and CO_2 on photosynthesis, growth, and elemental ratios in marine Synechococcus and Prochlorococcus (Cyanobacteria), J. Phycol., 43, 485–496, 2007.
Grossart, H. P., Allgaier, M., Passow, U., and Riebesell, U.: Testing the effect of CO_2 concentration on the dynamics of marine heterotrophic bacterioplankton, Limnol. Oceanogr., 51, 1–11, 2006.
Hönisch, B., Ridgwell, A., Schmidt, D. N., Thomas, E., Gibbs, S. J., Sluijs, A., Zeebe, R., Kump, L., Martindale, R. C., and Greene, S. E.: The geological record of ocean acidification, Science, 335, 1058–1063, 2012.
Hewson, I. and Fuhrman, J. A.: Improved strategy for comparing microbial assemblage fingerprints, Microb. Ecol., 51, 147–153, 2006.
Hutchins, D., Fu, F. X., Zhang, Y., Warner, M., Feng, Y., Portune, K., Bernhardt, P., and Mulholland, M.: CO_2 control of Trichodesmium N_2 fixation, photosynthesis, growth rates, and elemental ratios: implications for past, present, and future ocean biogeochemistry, Limnol. Oceanogr., 52, 1293–1304, 2007.
Hutchins, D. A., Mulholland, M. R., and Fu, F.: Nutrient cycles and marine microbes in a CO_2-enriched ocean, Oceanography, 22, 128–145, 2009.
IPCC: Climate Change 2007: Synthesis Report, Summary for policy makers, November, 2007.
Jiao, N., Herndl, G. J., Hansell, D. A., Benner, R., Kattner, G., Wilhelm, S. W., Kirchman, D. L., Weinbauer, M. G., Luo, T., and Chen, F.: Microbial production of recalcitrant dissolved organic matter: long-term carbon storage in the global ocean, Nat. Rev. Microbiol., 8, 593–599, 2010.
Joint, I., Doney, S. C., and Karl, D. M.: Will ocean acidification affect marine microbes?, ISME J., 5, 1–7, 2010.
Kirchman, D. L.: The ecology of *Cytophaga-Flavobacteria* in aquatic environments, FEMS Microbiol. Ecol., 39, 91–100, 2002.

BGD
9, 10645–10668, 2012

Lane, D.: 16S/23S rRNA sequencing, in: Nucleic Acid Techniques in Bacterial Systematics, edited by: Stackebrandt, E. and Goodfellow, M., John Wiley & Sons, New York, 115–175, 1991.

Lau, S. C. K., Thiyagarajan, V., Cheung, S. C. K., and Qian, P. Y.: Roles of bacterial community composition in biofilms as a mediator for larval settlement of three marine invertebrates, Aquat. Microb. Ecol., 38, 41–51, 2005.

Liu, J., Weinbauer, M. G., Maier, C., Dai, M., and Gattuso, J. P.: Effect of ocean acidification on microbial diversity and on microbe-driven biogeochemistry and ecosystem functioning, Aquat. Microb. Ecol., 61, 291–305, 2010a.

Liu, R., Chiang, M. H. Y., Lun, C. H. I., Qian, P. Y., and Lau, S. C. K.: Host-specific 16S rRNA gene markers of Bacteroidales for source tracking of fecal pollution in the subtropical coastal seawater of Hong Kong, Water Res., 44, 6164–6174, 2010b.

Martiny, J. B. H., Bohannan, B. J. M., Brown, J. H., Colwell, R. K., Fuhrman, J. A., Green, J. L., Horner-Devine, M. C., Kane, M., Krumins, J. A., and Kuske, C. R.: Microbial biogeography: putting microorganisms on the map, Nat. Rev. Microbiol., 4, 102–112, 2006.

Piontek, J., Lunau, M., Händel, N., Borchard, C., Wurst, M., and Engel, A.: Acidification increases microbial polysaccharide degradation in the ocean, Biogeosciences, 7, 1615–1624, doi:10.5194/bg-7-1615-2010, 2010.

Riebesell, U.: Effects of CO_2 enrichment on marine phytoplankton, J. Oceanogr., 60, 719–729, 2004.

Riebesell, U., Czerny, J., von Bröckel, K., Boxhammer, T., Büdenbender, J., Deckelnick, M., Fischer, M., Hoffmann, D., Krug, S. A., Lentz, U., Ludwig, A., Muche, R., and Schulz, K. G.: A mobile sea-going mesocosm system: New opportunities for ocean change research, Biogeosciences Discuss., accepted, 2012.

Schulz, K. G., Bellerby, R. G. J., Brussaard, C., Büdenbender, J., Czerny, J., Engel, A., Fischer, M., Koch Klavsen, S., Krug, S., Lischka, S., Ludwig, A., Meyerhöfer, M., Nondal, G., Silyakova, A., Stuhr, A., and Riebesell, U.: Temporal biomass dynamics of an Arctic plankton bloom in response to increasing levels of atmospheric carbon dioxide, Biogeosciences Discuss., accepted, 2012.

Zhang, R., Liu, B., Lau, S. C. K., Ki, J. S., and Qian, P. Y.: Particle-attached and free-living bacterial communities in a contrasting marine environment: Victoria Harbor, Hong Kong, FEMS Microb. Ecol., 61, 496–508, 2007.

BGD
9, 10645–10668, 2012

Table 1. BIOENV analysis of similarity matrices of bacterial community structure based on T-RFLP analysis and environmental factors. BIOENV analysis was performed for combined environmental factors to obtain the five highest ranked correlations between similarity matrices of community fingerprints and environmental data. The five individual environmental parameters with highest correlation values were also shown. DO: dissolved oxygen; BA: bacterial abundance; VBR: viruses-to-bacteria ratio; DMS: dimethylsulfide; PON: particulate organic nitrogen; POC: particulate organic carbon; A_T: total alkalinity.

Correlation	Combined environmental factors	Correlation	Single environmental factor
0.452	Salinity, DO, BA, VBR, DMS	0.305	Salinity
0.452	Salinity, DO, BA, VBR, PON	0.305	DO
0.450	Salinity, DO, BA, VBR, POC	0.294	BA
0.450	Salinity, DO, BA, VBR	0.265	A_T
0.445	Salinity, DO, BA, VBR, A_T	0.242	DMS

BGD
9, 10645–10668, 2012

Table 2. Major OTUs and clone numbers observed in clone library analysis. The phylogenetic assignment of each OTU was based on RDP Classifier and GenBank Blastn analysis.

OTUs	Phylogenetic assignment	M3 – 175 µatm	M2 – 250 µatm	M4 – 340 µatm	M8 – 425 µatm	M1 – 600 µatm	M6 – 675 µatm	M5 – 860 µatm	M9 – 1085 µatm	Total
Cryobacterium-like	*Actinobacteria*	16	30	19	18	57	6	14	13	173
Ilumatobacter	*Actinobacteria*	20	8	10	14	1	12	13	10	88
Owenweeksia	*Bacteroidetes*	2	1	3	0	0	0	1	1	8
Owenweeksia-like-1	*Bacteroidetes*	0	2	7	5	1	13	10	4	42
Owenweeksia-like-2	*Bacteroidetes*	7	0	1	0	0	0	0	1	9
Ulvibacter	*Bacteroidetes*	1	5	2	2	0	0	1	0	11
Polaribacter	*Bacteroidetes*	4	2	3	1	0	0	0	0	10
Fluviicola	*Bacteroidetes*	2	0	1	0	0	1	1	0	5
Haliscomenobacter	*Bacteroidetes*	3	0	2	2	0	2	3	0	12
Chlorophyta	*Cyanobacteria*	1	0	0	0	0	1	3	0	5
Sulfitobacter-1	*Proteobacteria* (α-)	0	2	1	4	0	0	0	4	11
Sulfitobacter-2	*Proteobacteria* (α-)	0	9	11	4	4	8	9	8	53
Loktanella	*Proteobacteria* (α-)	4	4	9	3	1	2	6	5	44
Pelagibacter	*Proteobacteria* (α-)	1	0	1	6	3	3	9	5	28
Octadecabacter	*Proteobacteria* (α-)	1	2	1	1	0	4	2	1	12
Hydrogenophaga-like	*Proteobacteria* (β-)	2	0	0	4	1	0	0	4	11
Methylophilus-1	*Proteobacteria* (β-)	6	0	2	5	0	6	1	6	26
Methylophilus-2	*Proteobacteria* (β-)	2	1	3	1	2	5	1	5	20
Haliea	*Proteobacteria* (γ-)	15	5	14	19	4	25	11	20	113
Gamma-1	*Proteobacteria* (γ-)	2	0	0	2	0	0	1	1	6
Gamma-2	*Proteobacteria* (γ-)	3	0	0	2	0	0	0	1	6
	Total	98	74	100	98	78	98	99	98	

BGD
9, 10645–10668, 2012

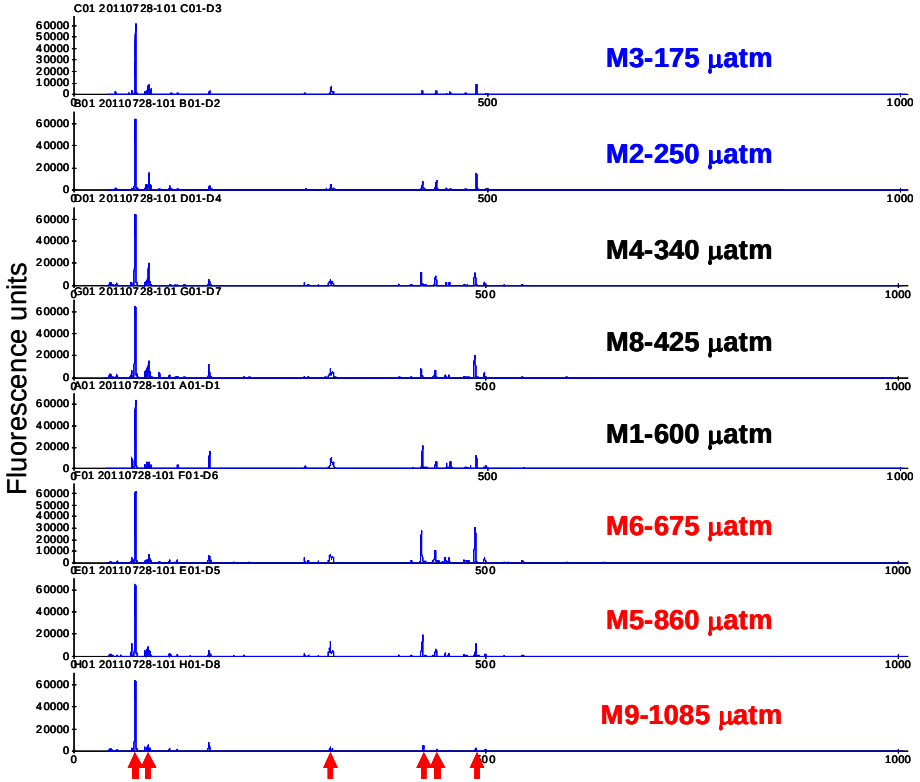

Fig. 1. Bacterial community structure of day 30 samples revealed using T-RFLP analysis. M7 sample is absent since the mesocosm was removed before day 30. Six T-RFs identified by in silico digestion of cloned 16S rRNA gene sequences are shown with red arrows (see Fig. 5 for their phylogenetic assignment).

BGD
9, 10645–10668, 2012

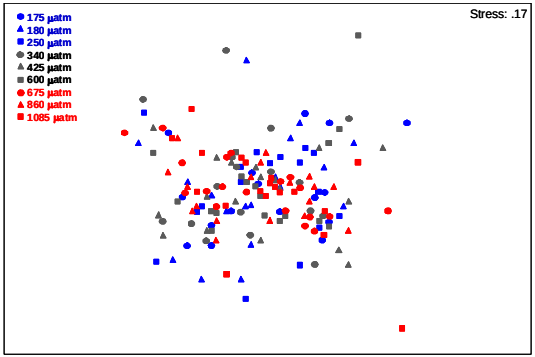

(a)

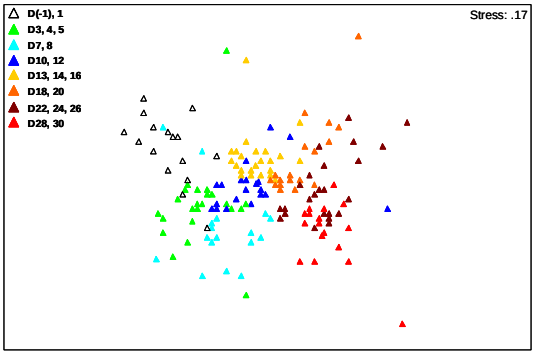

(b)

Fig. 2. MDS plots, based on double enzyme digested T-RFLP analysis, showing bacterial community dynamics during the ocean acidification mesocosm experiment. **(a)** displaying with mesocosm; **(b)** displaying with incubation time.

BGD
9, 10645–10668, 2012

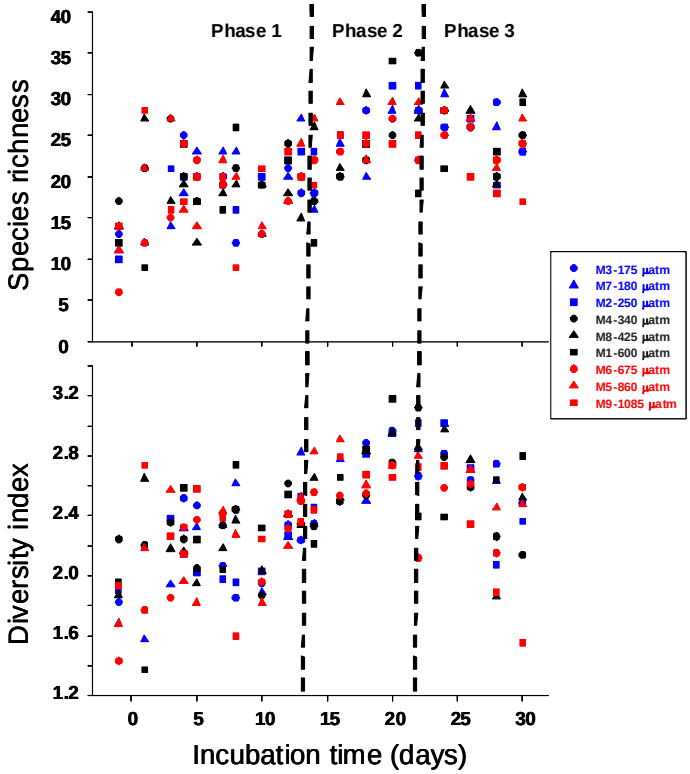

Fig. 3. Dynamics of bacterial species richness and diversity index during the ocean acidification mesocosm experiment revealed using T-RFLP analysis. Three phases of chl *a* concentrations during incubation are shown for reference. See Schulz et al. (2012).

BGD
9, 10645–10668, 2012

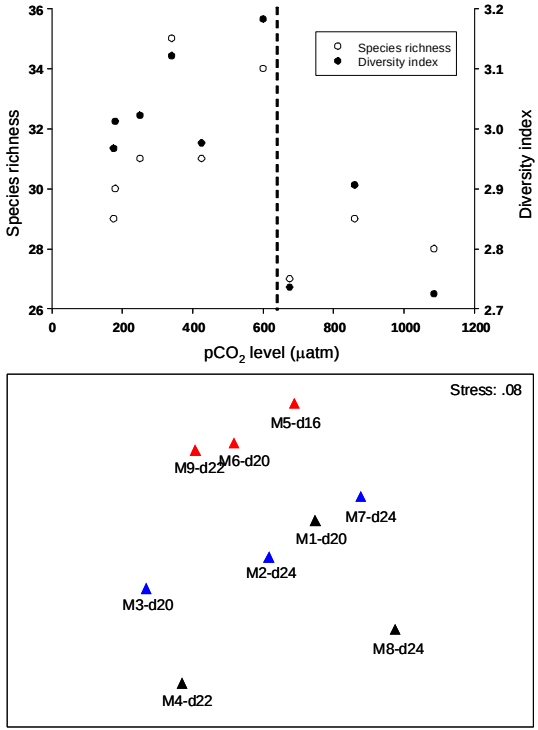

Fig. 4. Maximum bacterial species richness (S_{max}) and diversity index (H_{max}) during the ocean acidification mesocosm experiment revealed using T-RFLP analysis. The bacterial community structures of samples with S_{max} are shown on MDS plots. The possible biological threshold of ocean acidification effects is indicated by a dashed line.

BGD
9, 10645–10668, 2012

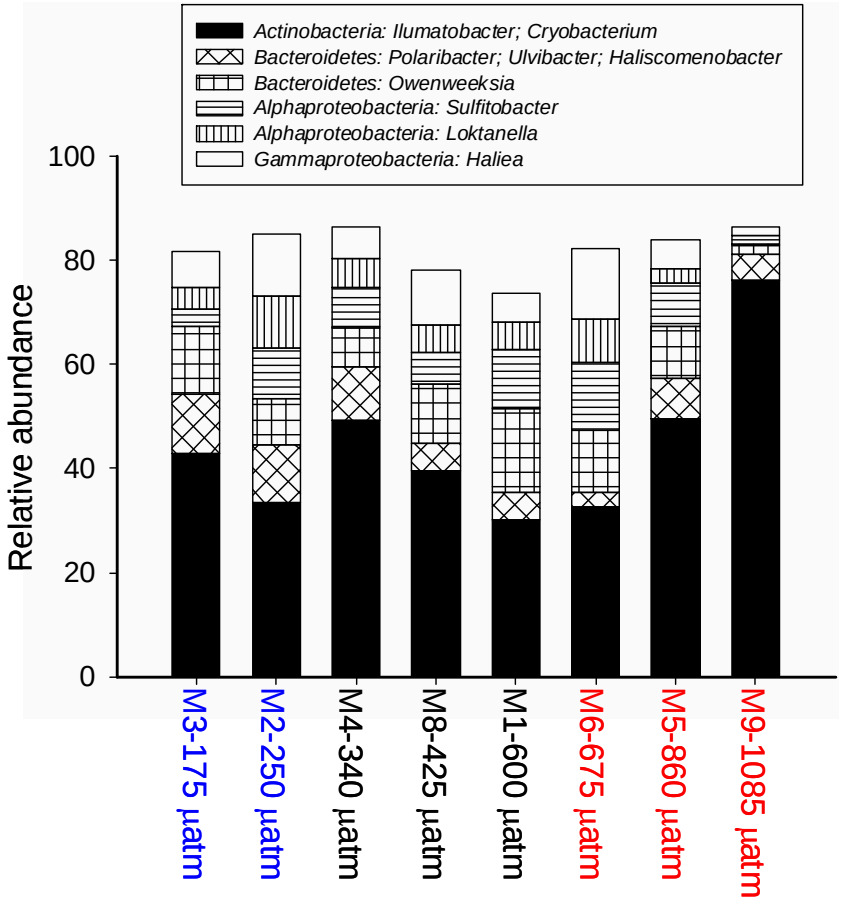

Fig. 5. Relative abundance of T-RFs identified using clone library analysis of eight mesocosms.

BGD
9, 10645–10668, 2012